

Research Article

Luminescent Solar Concentrators Fabricated by Dispersing Rare Earth Particles in PMMA Waveguide

Cheng Liu, Ruijiang Deng, Yanlin Gong, Cheng Zou, Yong Liu, Xiang Zhou, and Baojun Li

State Key Laboratory of Optoelectronic Materials and Technologies, School of Physics and Engineering, Sun Yat-Sen University, Guangzhou 510275, China

Correspondence should be addressed to Baojun Li; stslbj@outlook.com

Received 2 April 2014; Accepted 25 June 2014; Published 9 July 2014

Academic Editor: Harald Hoppe

Copyright © 2014 Cheng Liu et al. This is an open access article distributed under the Creative Commons Attribution License, which permits unrestricted use, distribution, and reproduction in any medium, provided the original work is properly cited.

Luminescent solar concentrators (LSCs) were fabricated by dispersing $\text{CaAlSiN}_3 : \text{Eu}^{2+}$ particles in a PMMA waveguide. A series of LSCs (dimension $5.0 \text{ cm} \times 5.0 \text{ cm} \times 0.5 \text{ cm}$) with different $\text{CaAlSiN}_3 : \text{Eu}^{2+}$ particle concentration were obtained and their performance was evaluated. The maximum optical concentration ratio is 1.23 with a power conversion efficiency of 1.44% for the LSC containing 0.5 wt% $\text{CaAlSiN}_3 : \text{Eu}^{2+}$ particles concentration. This strategy of dispersing rare earth particles in PMMA waveguide represents an alternative approach to producing highly durable LSCs.

1. Introduction

Luminescent solar concentrators (LSCs) were introduced in the 1970s as an approach to lowering the costs of solar power [1]. Such LSCs have received great interest recently because of their potential for achieving high optical concentration ratios without tracking the sun [2–5]. Waveguide-based LSCs can absorb short wavelength sunlight and then reemit it at longer wavelengths. A large fraction of the emitted light is trapped in the waveguide through total internal reflection and concentrated toward small solar cells attached to the edges of the waveguide. To date, numerous types of luminescent materials have been developed and tested for use in LSCs, including organic dyes [6, 7], quantum dots [8, 9], and rare earth materials [10–13]. However, both organic dyes and quantum dots suffer from self-absorption caused by overlap between their absorption and emission bands. This limits the optical concentration ratios of such LSCs to approximately one. Compared with organic dyes and quantum dots, rare earth materials feature large Stokes shifts between their absorption and emission bands and have considerable promise for applications in LSC. Among such rare earth materials, $\text{CaAlSiN}_3 : \text{Eu}^{2+}$ emits wavelength in the range of 600–700 nm, which can be efficiently absorbed by solar cells. This material combines the excellent chemical stability of nitridosilicates with the unique luminescent features of

Eu^{2+} ions including (1) a broad absorption bandwidth to utilize the solar spectrum efficiently, (2) large Stokes shift to minimize overlap of the absorption and emission spectral that lead to self-absorption losses, and (3) high fluorescent quantum yield [14, 15]. These features are particularly desirable for producing efficient and durable LSCs. Poly(methyl methacrylate) (PMMA) is a typical waveguide material with high transparency (92% for visible light) and a high refractive index ($n = 1.49$) that can also be easily processed [16]. In this work, LSCs were fabricated, consisting of a PMMA waveguide dispersed with $\text{CaAlSiN}_3 : \text{Eu}^{2+}$ particles using a modified procedure that was previously used to form a CdSe/ZnS quantum dot-PMMA composite [17]. The performance of the LSCs was investigated experimentally and compared with corresponding LSCs based on organic dyes and quantum dots.

2. Experiment

2.1. Fabrication of LSCs. LSCs were prepared with fixed dimensions of $5.0 \text{ cm} \times 5.0 \text{ cm} \times 0.5 \text{ cm}$ and varying concentration of $\text{CaAlSiN}_3 : \text{Eu}^{2+}$ particles. These particles were purchased from a commercial supplier (Grirem Advanced Materials, China) with a quantum efficiency of 83% and an absorption efficiency of 92%. The particle size ranges

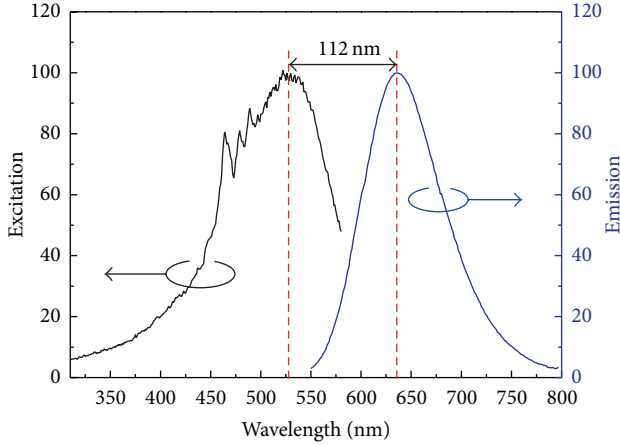


FIGURE 1: Excitation and emission of the $\text{CaAlSiN}_3:\text{Eu}^{2+}$ particles with a Stokes shift of 112 nm.

from 5 to 30 μm with an average diameter of 11 μm . The excitation and emission spectra of the particles are shown in Figure 1. To fabricate the LSC, the $\text{CaAlSiN}_3:\text{Eu}^{2+}$ particles were first dispersed in a methyl methacrylate (MMA) monomer solution by ultrasonic stirring. During the stirring, azobisisobutyronitrile (AIBN) was added to the solution at an AIBN/MMA weight ratio of 0.1 wt%. The mixture was heated to 90°C using a thermostatic water bath for 30 min to complete prepolymerization and then cooled to room temperature. The solution was poured into molds (0.5 cm thick) and then placed in an oven at 50°C for longer than 20 hours for postpolymerization. The oven temperature was increased to 100°C for 1 hour to complete polymerization. Finally, the as-prepared 0.5 cm thick PMMA plates were cut into LSCs with areas of 5 cm \times 5 cm by laser cutting. By controlling the $\text{CaAlSiN}_3:\text{Eu}^{2+}$ particles concentration, a series of LSCs were fabricated at 0.10 wt%, 0.25 wt%, 0.50 wt%, 1.00 wt%, and 2.00 wt%. Figure 2 shows photographs of a LSC containing $\text{CaAlSiN}_3:\text{Eu}^{2+}$ particle concentration of 0.5 wt%. An optical microscope image (Figure 2(a)) of the LSC shows that the particles (an individual particle is indicated by a red circle) are randomly dispersed in the PMMA matrix without agglomeration. Figures 2(b) and 2(c) show photographs of the LSC illuminated by ambient and ultraviolet (UV) light, respectively. Excitation by UV light results in strong red emission.

2.2. Performance Evaluation of LSCs. To evaluate the performance of LSCs with different $\text{CaAlSiN}_3:\text{Eu}^{2+}$ particle concentration, a sample holder was fabricated, shown in Figure 3(a). The sample holder contains three adjustable support brackets mounted with normal silver mirrors (>95% reflectance) and a back mirror (dimension 5 cm \times 5 cm). During measurement, a laser cut monocrystalline silicon (c-Si) solar cell (5 cm \times 0.5 cm) was attached to the output edge of the LSC before being placed in the sample holder (see Figure 3(b)). By illuminating the LSC using a solar

simulator (Newport's Oriel 91192) under AM 1.5 conditions (100 mW/cm^2) as shown schematically in Figure 4(a), the current-voltage (I - V) curve of the attached solar cell was measured via a source meter (Keithley 2400). Figure 4(b) shows the I - V curves of the solar cell attached to LSCs with $\text{CaAlSiN}_3:\text{Eu}^{2+}$ particle concentration of 0.10, 0.25, 0.50, 1.00, and 2.00 wt%. For comparison, the I - V curve of the solar cell illuminated directly by the solar simulator is also given in Figure 4(b) (dashed black line) indicating a conversion efficiency of 11.70%, a short circuit current of 84.83 mA, and an open circuit voltage of 0.55 V. According to the I - V curves of the solar cell, electrical power output of the solar cell as a function of the voltage was obtained (Figure 5) and the maximum electrical power output (P_{out}) was found out, which reflects the light output at the edge of the LSC. The relationship between P_{out} and the $\text{CaAlSiN}_3:\text{Eu}^{2+}$ particle concentration of the LSCs is plotted in Figure 5 inset. As $\text{CaAlSiN}_3:\text{Eu}^{2+}$ particle concentration increases, P_{out} reaches a maximum of 36.04 mW at 0.5 wt%, before declining.

3. Results and Discussion

Power conversion efficiency (η_{PCE}) relates to the electrical power output from the solar cell attached to LSC in relation to the incident light power on the top surface of the LSC. The concentration ratio (C) is defined as the ratio between incoming and outgoing optical radiance. η_{PCE} and C are given by

$$\eta_{\text{PCE}} = \frac{P_{\text{out}}}{P_{\text{in}}}, \quad (1)$$

$$C = G \frac{P_{\text{out}}}{P_{\text{in}}\eta_0},$$

where G is the geometric gain which means the ratio of LSC illuminated surface area to the area of the edge where the solar cell is attached, P_{in} is the incident light power on the top surface of the LSC, P_{out} is the electrical power output measured from the solar cell attached to the LSC, and η_0 is the bare cell conversion efficiency. In our case, $G = 10$, $\eta_0 = 11.70\%$, $P_{\text{in}} = 2.5 \text{ W}$ (100 $\text{mW}/\text{cm}^2 \times (5 \times 5 \text{ cm}^2)$), and P_{out} varies with the $\text{CaAlSiN}_3:\text{Eu}^{2+}$ particle concentration dispersed in LSCs with a maximum value of 36.04 mW at a particle concentration of 0.5 wt% (see Section 2.2). The highest power conversion efficiency calculated from (1) is $\eta_{\text{PCE}} = 1.44\%$, with an optical concentration ratio of $C = 1.23$. This indicates the electrical power output of the solar cell attached to LSC increases to 123% of that of the bare cell. The concentration of the $\text{CaAlSiN}_3:\text{Eu}^{2+}$ influences the performance of LSCs. For the particle concentration of less than 0.5 wt%, the efficiency of the LSCs increases with the increasing particle concentration because more solar photons are absorbed by the LSCs. For the particle concentration of greater than 0.5 wt%, the efficiency decreases with the increasing particle concentration, because the increasing particle concentration results in greater self-absorption and scattering loss. So, the LSC with a particle concentration of 0.5 wt% exhibits the best performance.

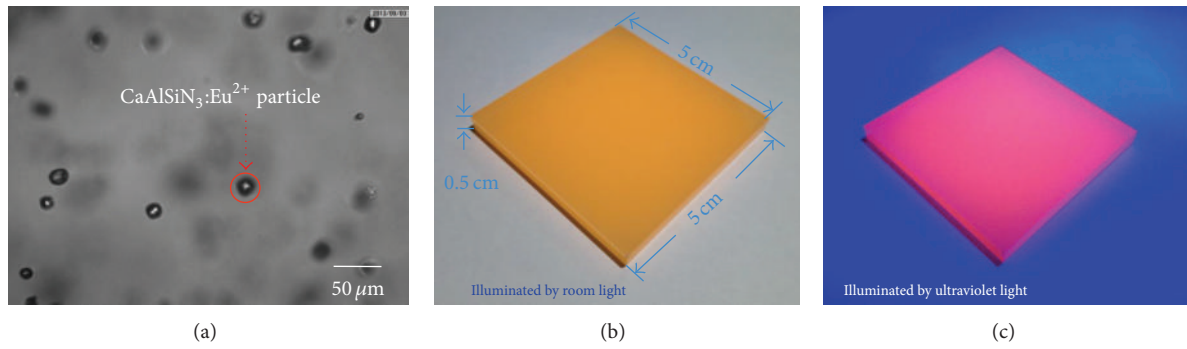


FIGURE 2: (a) Optical microscope image of an LSC with a CaAlSiN₃:Eu²⁺ particle concentration of 0.5 wt%. Photographs of an LSC illuminated by (b) ambient light and (c) UV light.

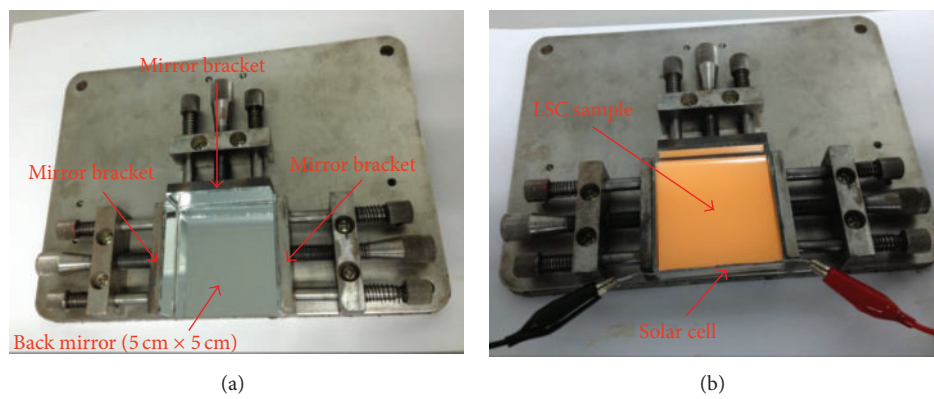


FIGURE 3: (a) Photo of sample holder. (b) The sample holder with a LSC mounted. The output edge of the LSC is fitted with a solar cell.

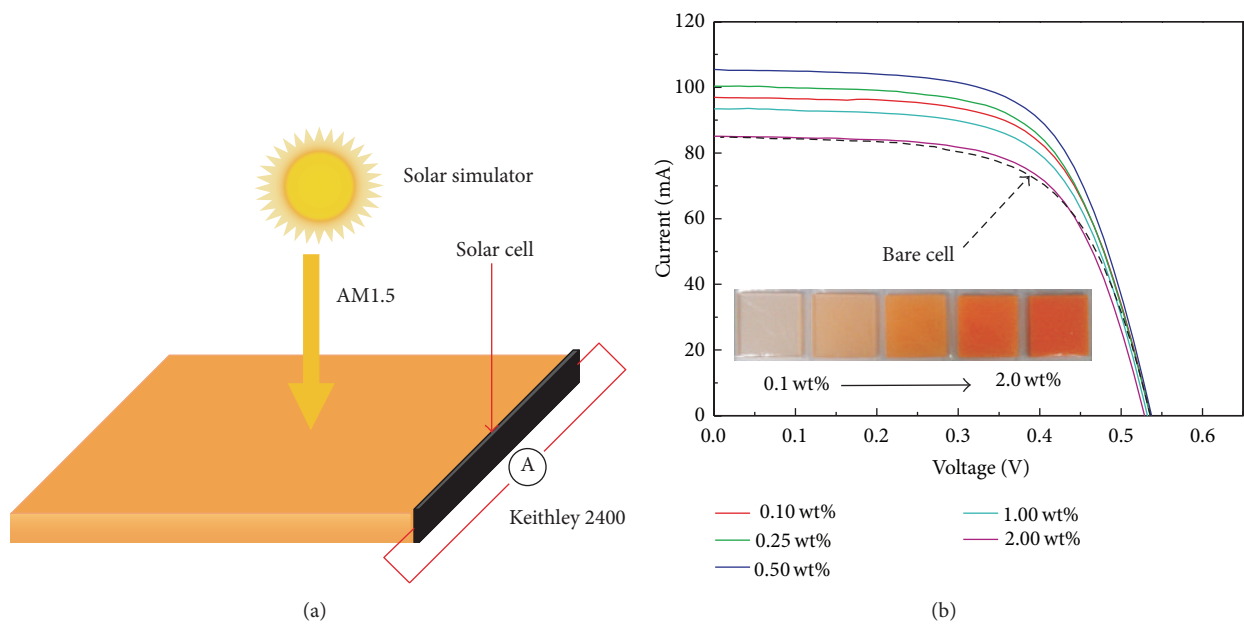


FIGURE 4: (a) Scheme of the measurement setup. (b) *I-V* curves of the solar cell attached to LSCs with different CaAlSiN₃:Eu²⁺ particle concentration. The dashed black line shows the *I-V* curve of the bare cell illuminated directly by the solar simulator. The inset shows photographs of LSCs with increasing particle concentration from left to right.

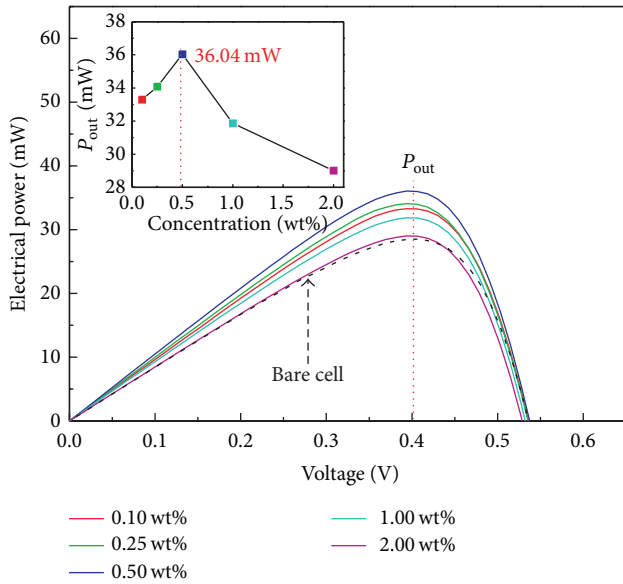


FIGURE 5: Electrical power output of the solar cell attached to LSCs. The dashed black line shows electrical power output of the bare cell. The maximum electrical power P_{out} is plotted against the particle concentration as shown in the inset.

The C and η_{PCE} of an LSC depend strongly on the LSC dimensions and the number and type of solar cells attached. For a $5\text{ cm} \times 5\text{ cm}$ sized LSCs based on commercial quantum dots (for the same case of a single mc-Si solar cell attached to the LSC), typically reported η_{PCE} values are generally below 0.5% and the highest C values are below one [9, 18]. Our best result of $\eta_{PCE} = 1.44\%$ represents a 3-fold increase over the reported values ($\eta_{PCE} \approx 0.5\%$). Although this result is less than the highest reported values for similar LSC systems based on organic dyes ($\eta_{PCE} = 2.9\%$, with $C \approx 1.7$) [6], $\text{CaAlSiN}_3 : \text{Eu}^{2+}$ particles have greater chemical stability than organic dyes, which may lead to a more durable LSC. In addition, the theoretical limit of the concentration ratio for an LSC is related to the Stokes shift, by $C_{lim} \approx (e_{em}^3/e_{abs}^3) \times \exp[(e_{abs} - e_{em})/k_B T]$, where e_{abs} and e_{em} are the absorbed and emitted photon energies, respectively [19]. The larger Stokes shift reduces the self-absorption loss and allows for a higher concentration ratio. In this work, the excitation and emission band of the $\text{CaAlSiN}_3 : \text{Eu}^{2+}$ particles feature a larger Stokes shift (112 nm, see Figure 1) than the typical for organic dyes ($\approx 25\text{ nm}$ for Red305 dye [7]). This contributes to lower loss through self-absorption in the waveguide structure of LSCs. So, theoretically, LSCs using $\text{CaAlSiN}_3 : \text{Eu}^{2+}$ particles should have better performance than those based on organic dyes. However, unlike organic dyes, these inorganic particles are not fully miscible with the MMA monomer during the fabrication and have size greater than the wavelength of visible light. This may lead to partial scattering of light out of the waveguide structure, lowering the performance of the LSCs. To improve the LSC performance, scattering loss could be reduced by using nanosized particles or matching the refractive index of the waveguide matrix to that of the $\text{CaAlSiN}_3 : \text{Eu}^{2+}$ particles [12].

4. Conclusion

Using $\text{CaAlSiN}_3 : \text{Eu}^{2+}$ particles, we demonstrated a strategy for dispersing rare earth particles in a PMMA waveguide for use in LSCs. The highest optical concentration ratio we measured is $C = 1.23$, with a η_{PCE} of 1.44% for a $5\text{ cm} \times 5\text{ cm}$ -LSC with a $\text{CaAlSiN}_3 : \text{Eu}^{2+}$ particle concentration of 0.5 wt%. Although the experiments were carried out using $\text{CaAlSiN}_3 : \text{Eu}^{2+}$ particles, this strategy may be extended to other rare earth particle systems. This work demonstrates that dispersing rare earth particles in PMMA waveguides is a promising approach to generating high performance LSCs.

Conflict of Interests

The authors declare that there is no conflict of interests regarding the publication of this paper.


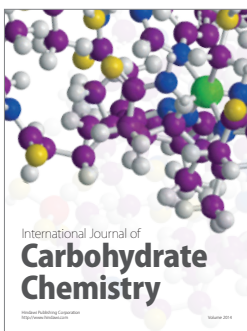
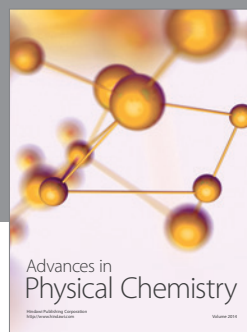
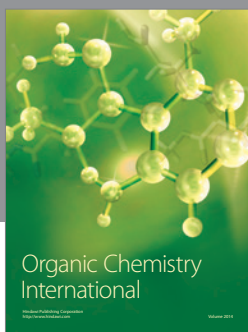
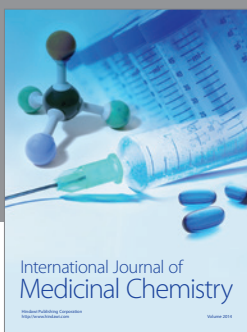
Acknowledgments

This work was supported by the National Basic Research Program of China (973 Program no. 2012CB933704), the National Natural Science Foundation of China (no. 11274395), and the Program for Changjiang Scholars and Innovative Research Team in University (IRT13042).

References

- [1] A. Goetzberger and V. Wittwer, "Fluorescent planar collector-concentrators: a review," *Solar Cells*, vol. 4, no. 1, pp. 3–23, 1981.
- [2] M. J. Currie, J. K. Mapel, T. D. Heidel, S. Goffri, and M. A. Baldo, "High-efficiency organic solar concentrators for photovoltaics," *Science*, vol. 321, no. 5886, pp. 226–228, 2008.
- [3] N. C. Giebink, G. P. Wiederrecht, and M. R. Wasielewski, "Resonance-shifting to circumvent reabsorption loss in luminescent solar concentrators," *Nature Photonics*, vol. 5, no. 11, pp. 694–701, 2011.
- [4] M. G. Debije and P. P. C. Verbunt, "Thirty years of luminescent solar concentrator research: solar energy for the built environment," *Advanced Energy Materials*, vol. 2, no. 1, pp. 12–35, 2012.
- [5] C. Chou, J. Chuang, and F. Chen, "High-performance flexible waveguiding photovoltaics," *Scientific Reports*, vol. 3, article 2244, 2013.
- [6] L. H. Slooff, E. E. Bende, A. R. Burgers et al., "A luminescent solar concentrator with 7.1% power conversion efficiency," *Physica Status Solidi—Rapid Research Letters*, vol. 2, no. 6, pp. 257–259, 2008.
- [7] L. Desmet, A. J. M. Ras, D. K. G. de Boer, and M. G. Debije, "Monocrystalline silicon photovoltaic luminescent solar concentrator with 4.2% power conversion efficiency," *Optics Letters*, vol. 37, no. 15, pp. 3087–3089, 2012.
- [8] G. V. Shcherbatyuk, R. H. Inman, C. Wang, R. Winston, and S. Ghosh, "Viability of using near infrared PbS quantum dots as active materials in luminescent solar concentrators," *Applied Physics Letters*, vol. 96, no. 19, Article ID 191901, 2010.
- [9] S. J. Gallagher, B. Norton, and P. C. Eames, "Quantum dot solar concentrators: electrical conversion efficiencies and comparative concentrating factors of fabricated devices," *Solar Energy*, vol. 81, no. 6, pp. 813–821, 2007.

- [10] R. Reisfeld and Y. Kalisky, "Improved planar solar converter based on uranyl neodymium and holmium glasses," *Nature*, vol. 283, no. 5744, pp. 281–282, 1980.
- [11] T. Wang, J. Zhang, W. Ma et al., "Luminescent solar concentrator employing rare earth complex with zero self-absorption loss," *Solar Energy*, vol. 85, no. 11, pp. 2571–2579, 2011.
- [12] D. K. G. de Boer, D. J. Broer, M. G. Debije et al., "Progress in phosphors and filters for luminescent solar concentrators," *Optics Express*, vol. 20, no. 103, pp. A395–A405, 2012.
- [13] X. Wang, T. Wang, X. Tian et al., "Europium complex doped luminescent solar concentrators with extended absorption range from UV to visible region," *Solar Energy*, vol. 85, no. 9, pp. 2179–2184, 2011.
- [14] K. Uheda, N. Hirosaki, Y. Yamamoto, A. Naito, T. Nakajima, and H. Yamamoto, "Luminescence properties of a red phosphor, $\text{CaAlSiN}_3:\text{Eu}^{2+}$, for white light-emitting diodes," *Electrochemical and Solid-State Letters*, vol. 9, no. 4, pp. H22–H25, 2006.
- [15] J. Yang, T. Wang, D. Chen, G. Chen, and Q. Liu, "An investigation of Eu^{2+} -doped CaAlSiN_3 fabricated by an alloy-nitridation method," *Materials Science and Engineering B*, vol. 177, no. 18, pp. 1596–1604, 2012.
- [16] M. J. Kastelijn, C. W. M. Bastiaansen, and M. G. Debije, "Influence of waveguide material on light emission in luminescent solar concentrators," *Optical Materials*, vol. 31, no. 11, pp. 1720–1722, 2009.
- [17] L. Pang, Y. Shen, K. Tetz, and Y. Fainman, "PMMA quantum dots composites fabricated via use of pre-polymerization," *Optics Express*, vol. 13, no. 1, pp. 44–49, 2005.
- [18] V. Sholin, J. D. Olson, and S. A. Carter, "Semiconducting polymers and quantum dots in luminescent solar concentrators for solar energy harvesting," *Journal of Applied Physics*, vol. 101, no. 12, Article ID 123114, 2007.
- [19] G. Smestad, H. Ries, R. Winston, and E. Yablonoitch, "The thermodynamic limits of light concentrators," *Solar Energy Materials*, vol. 21, no. 2, pp. 99–111, 1990.



Hindawi

Submit your manuscripts at
<http://www.hindawi.com>

